

**High-Density Photogenerated Free-Carrier Spin
Relaxation Processes in Wurtzite Semiconductors: CdSe
and Semimagnetic Semiconductor $\text{Cd}_{1-x}\text{Mn}_x\text{Se}$**

Mahesh R. Junnarkar

R. R. Alfano

J. K. Furdyna

Reprinted from
IEEE JOURNAL OF QUANTUM ELECTRONICS
Vol. 24, No. 2, February 1988

High-Density Photogenerated Free-Carrier Spin Relaxation Processes in Wurtzite Semiconductors: CdSe and Semimagnetic Semiconductor $Cd_{1-x}Mn_xSe$

MAHESH R. JUNNARKAR, R. R. ALFANO, AND J. K. FURDYNA

Abstract—Picosecond time-resolved spin relaxation kinetics of high-density free carriers is investigated at low temperatures in CdSe ($x = 0$) and in dilute semimagnetic semiconductor $Cd_{1-x}Mn_xSe$ for $x = 0.05$ and 0.10 . The fast spin relaxation observed in CdSe results from a mechanism associated with the noncentrosymmetric character of the band structure for this material. This process is similar to the one proposed by D'yakonov and Perel' (D-P) for the zinc blende crystal structures. The spin relaxation times in CdSe are on the order of 30 ps and are independent of the laser power within the range of photon flux of 1.29×10^{24} – $4.25 \times 10^{27}/cm^2 \cdot s$. This is believed to arise from the fast diffusion of carriers from the photoexcited region which limits the maximum carrier density to $\sim 5 \times 10^{18}/cm^3$. The observed spin polarization factor for carriers in CdSe is in good agreement with theory. The spin relaxation times are < 20 ps in semimagnetic semiconductor $Cd_{1-x}Mn_xSe$ and are consistent with spin flip Raman scattering measurements. The increase in spin relaxation rate relative to CdSe is explained in terms of the carrier spin exchange between the carriers and the magnetic spin sites. The carrier spin exchange with magnetic spin sites and the D-P process inherent in the host crystal are equally important in semimagnetic semiconductors. The spin polarization factor $\rho_1(0)$ obtained in CdSe is ~ 50 percent using one-photon excitation, while for $Cd_{0.95}Mn_{0.05}Se$ and $Cd_{0.9}Mn_{0.1}Se$, the values ($\rho_2(0)$) are ≈ 18 and ≈ 28 percent using two-photon excitation. A probable cause for the reduction in the observed spin polarization factor for carriers in $Cd_{1-x}Mn_xSe$ ($x \neq 0$) is presented.

INTRODUCTION

AN EFFICIENT source [1] of spin-polarized electrons is of technological interest for high-energy scattering, low-energy electron diffraction, and atomic scattering. The generation of spin-oriented carriers in the conduction band by "polarized optical pumping" from heavy hole and light hole valence bands has been known [2], [3] for over two decades. Measurements of the spin relaxation rates in semiconductors are important for understanding the basic physics behind carrier spin interaction and

scattering mechanisms. The dipole allowed optical selection rules govern the maximum degree of spin polarization of carriers in semiconductors. In zinc blende structures, the optical transition from the valence bands Γ_8 to the conduction band Γ_6 are such that there are three times as many electrons excited to a state with spin anti-parallel to the excitation photon angular momentum as compared to the spin parallel to it [4]. A similar situation arises for the semimagnetic semiconductor $Cd_{1-x}Mn_xSe$ ($0 \leq x < 0.5$) having a wurtzite lattice, even though the conduction band and valence bands are of Γ_7 and Γ_9 , Γ_7 group symmetry [5], respectively. The steady-state spin polarization of the conduction electrons depends not only on the selection rules (or the symmetry of the crystal structure), but also on the relaxation mechanisms [4]–[10]. Various laboratories have investigated [9]–[12] the mechanisms of spin relaxation. Most of the work performed in this field has been confined to the study of GaAs with cubic symmetry, and the experimental techniques to obtain information on spin relaxation rates are indirect such as the Hanle effect [10], [13], electron spin resonance [14], and spin-flip Raman scattering [15], [16]. Using a streak camera, we have previously made the first real-time measurements [11], [17] of the spin relaxation rates of high-density photogenerated carriers in GaAs. To date, no real-time spin polarization kinetics have been studied in semimagnetic semiconductors.

Over the past three years, semimagnetic semiconductors have attracted a lot of attention because of their fascinating and useful [18] electronic, magnetic, and optical properties, i.e., large magnetooptic effect, large spin-flip Raman shifts, etc. These effects are due to the strong exchange interaction of carriers with the localized Mn^{2+} ions.

In this paper, we continue our previous research [11], [17] on spin relaxation mechanisms and direct our investigation to the transient spin effects in the II–VI wurtzite CdSe and the semimagnetic semiconductor $Cd_{1-x}Mn_xSe$ for $x = 0.05$ and 0.1 . These samples were chosen for spin relaxation experiments to investigate the spin exchange mechanism [18]. The experimental data are interpreted in terms of two spin relaxation mechanisms proposed by D'yakonov and Perel' [6]. The first mechanism of spin relaxation relates the relaxation rate to the noncentrosym-

Manuscript received May 4, 1987; revised September 10, 1987. This work was supported by the National Science Foundation under Grant DMR-840-4932, by the U.S. Air Force Office of Scientific Research under Grant AFOSR-860031 at the City College of New York, and by the National Science Foundation under MRL Grant DMR-83-16988 at Purdue University.

M. R. Junnarkar and R. R. Alfano are with the Institute for Ultrafast Spectroscopy and Lasers, Department of Physics and Electrical Engineering, City College of New York, New York, NY 10031.

J. K. Furdyna was with the Department of Physics, Purdue University, West Lafayette, IN 47907. He is now with the Department of Physics, University of Notre Dame, Notre Dame, IN 46556.

IEEE Log Number 8717847.

metric nature of the host crystal (CdSe), while the second mechanism addresses the effect of the exchange interaction between carrier spins and localized magnetic spins. Other mechanisms, particularly the one proposed by Elliot and Yafet [7], [10], are discarded because of the tenfold slower kinetics.

BACKGROUND

The host crystal CdSe is a II-VI semiconductor with wurtzite crystal structure [5]. The valence bands consist of the A , B , and C bands having Γ_9 , Γ_7 , and Γ_7 symmetry at $k = 0$, respectively (Fig. 1). The anisotropic crystal field in hexagonal crystals leads to lifting of the degeneracy at $k = 0$ and to the splitting of the upper valence bands Γ_8 into subbands Γ_{9A} and Γ_{7B} . This is in contrast to the cubic crystals such as GaAs. The conduction band has Γ_7 symmetry having a direct bandgap above Γ_{9A} of 1.84 eV at 4 K. The energy splitting $\Gamma_{9A} - \Gamma_{7B}$, corresponding to the crystal field, is 26.3 meV, and that of the split-off energy $\Gamma_{7B} - \Gamma_{7C}$, corresponding to the spin orbit interaction, is 406 meV [5].

For single-photon absorption, the selection rules are as follows: the transition from the Γ_{9A} valence band to the Γ_7 conduction band is allowed for light polarized $E \perp C$ (c axis of symmetry), and transitions from the valence bands Γ_{7B} , Γ_{7C} to the Γ_7 conduction band are allowed for light polarized $E \perp C$ and $E \parallel C$. For the absorption with circularly polarized light propagating along the c axis, the selection rules yield the same spin-polarized carrier population ratio in the conduction band as for cubic crystals [5]. $\text{Cd}_{1-x}\text{Mn}_x\text{Se}$, within the range of manganese atomic concentration $0 \leq x \leq 0.45$, has the wurtzite of crystal structure. The selection rules are identical to those in the host CdSe lattice.

The spin polarization factor $\rho(t)$ is defined by

$$\rho(t) = \frac{N\uparrow(t) - N\downarrow(t)}{N\uparrow(t) + N\downarrow(t)} \quad (1)$$

where $N\uparrow(t)$ and $N\downarrow(t)$ are the spin densities of electrons at time t with spin $1/2$ and $-1/2$, respectively. The rate equations for the polarized carriers in terms of the total recombination lifetime τ and spin relaxation time T_s after a δ pulse excitation are given by

$$\frac{dN\uparrow}{dt} = -\frac{N\uparrow}{\tau} - \frac{N\uparrow}{T_s} + \frac{N\downarrow}{T_s} \quad (2)$$

and

$$\frac{dN\downarrow}{dt} = -\frac{N\downarrow}{\tau} - \frac{N\downarrow}{T_s} + \frac{N\uparrow}{T_s} \quad (3)$$

The solution of these equations gives the time-dependent polarization factor

$$\rho(t) = \rho(0) \exp[-t/(T_s/2)] \quad (4)$$

where $\rho(0)$ is the selection rule allowed polarization factor. For one-photon absorption [4], $\rho(0)$ turns out to be 50 percent, while for two-photon absorption [22], $\rho(0)$ is

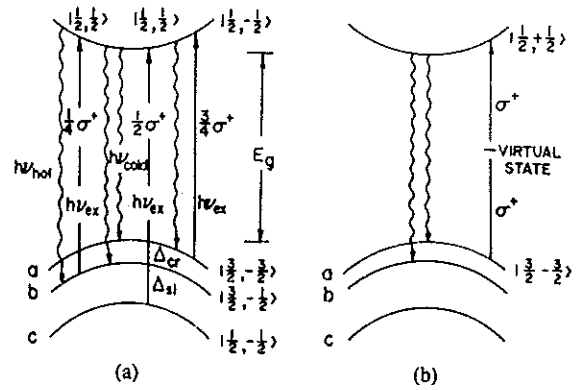


Fig. 1. (a) One-photon transitions from valence bands A , B , C to the conduction band for a wurtzite semiconductor. The relative transition probabilities are shown. The spin densities involve addition of various transitions with weighted density of states. In (b), the simple two-photon absorption model is shown. The two-photon absorption predicts 100 percent spin polarization unless band mixing is taken into account. The straight arrows correspond to absorption, while wiggled arrows show photoluminescence.

100 percent. Of course, these values are reduced from the maximum values because of band mixing. The transitions from split-off valence band tend to decrease the initial spin polarization. The effect of our experimental situation will be discussed later (see Discussion). If we assume that the holes depolarize very fast [19] ($\sim 10^{-13}$ s), the luminescence polarization factor, which is given by

$$L(t) = \frac{\sigma^+(t) - \sigma^-(t)}{\sigma^+(t) + \sigma^-(t)} \quad (5)$$

is equal to $\rho(t)$. $\sigma^+(t)$ and $\sigma^-(t)$ are luminescence intensities for right and left circular polarization at time t .

The recombination lifetime is obtained by adding (2) and (3) as follows:

$$\frac{dN}{dt} = \frac{dN\uparrow}{dt} + \frac{dN\downarrow}{dt} \quad (6)$$

Hence,

$$N(t) = N(0) e^{-t/\tau} \quad (7)$$

where $N(0)$ is the carrier density at $t = 0$.

SAMPLES

The samples of CdSe (high resistivity and low resistivity) were acquired from Cleveland Crystals, Inc. All the samples used in this experiment have the c axis perpendicular to the flat face ($\pm 2^\circ$).

The samples of $\text{Cd}_{1-x}\text{Mn}_x\text{Se}$ used were grown at Purdue University by the Bridgeman method. Both the samples ($x = 0.05$ and 0.1) are background doped with In ($\sim 10^{16}/\text{cm}^3$). The sample geometry is similar to the CdSe crystals and was described earlier. The propagation vector K of the excitation photon is oriented parallel to the c axis.

EXPERIMENTAL METHOD

Samples were mounted on a cold finger in a liquid He dewar with optical windows. The temperature was mon-

itored using a Si diode. Photoexcited carriers were produced using a Nd:glass laser mode locked by Kodak A9860 dye dissolved in dichloroethane. Single-pulse (6 ps) two-photon excitation ($\lambda = 1060$ nm) was achieved using a spark gap and a Pockel cell for pulse selection from the mode-locked train. The details of the time-resolved spin-polarized photoluminescence setup and picosecond laser system have been described elsewhere [17], [20]. The single-photon excitation ($\lambda = 530$ nm) was carried out using second harmonic generation in KDP. Stokes-shifted stimulated Raman photon excitation at 623 nm was achieved using a frequency-doubled pulse (530 nm) passing through ethanol.

The linearly polarized output of the laser system was circularly polarized (left or right) before excitation, and the circularly polarized (left or right) luminescence from the samples was analyzed using a broad-band quarter-wave plate. A Wollaston prism was placed in front of the entrance slit of a streak camera to spatially resolve the left and right circular polarization of the luminescence. A weak laser prepulse (530 nm) was directed into the entrance slit of the streak camera prior to the arrival of luminescence. This prepulse (see Figs. 2–7) was used as a marker for overlapping various data files for averaging, adding and subtracting. Thus, single-shot kinetics for left and right circular polarization of the luminescence was investigated simultaneously. The electronic windows set on a video camera controlled by a microprocessor enabled us to record and store the data [21] in a minicomputer. The intensity and time axis of the measured temporal curves displayed in Figs. 2–7 are corrected for the streak rate nonlinearity of the streak camera. The temporal resolution-laser pulse FWHM of the streak camera is 13 ps. This correspondence to total experimental time resolution. The luminescence bands were selected using dielectric filters in front of the streak camera.

In order to measure $\rho(t)$, it is necessary to calibrate the intensity ratio between the two windows. Under the most ideal condition, the windows are properly balanced and the ratio is equal to unity. In some cases, this is not so; then the ratio was determined and used as a correction factor. To obtain this correction factor, we used linearly polarized excitation. The luminescence from a sample in such a case would be equally circularly polarized ($I_{\sigma^+} = I_{\sigma^-}$), while the recorded data in the two windows would reflect the imbalance of the intensity response. Using this information, all the subsequent time-resolved photoluminescence data for circularly polarized excitation were corrected for the different window sensitivity. Using (4), (5), and (7), we deduced the values of $\rho(0)$, T_s , and τ .

EXPERIMENTAL RESULTS

A. CdSe

Experiments on CdSe were carried out at 77 K. Fig. 2 shows spin-polarized time-resolved luminescence for one-photon 530 nm and σ^+ polarization pumping. The curves (a) and (b) in Fig. 2 correspond to σ^+ and σ^- polarization

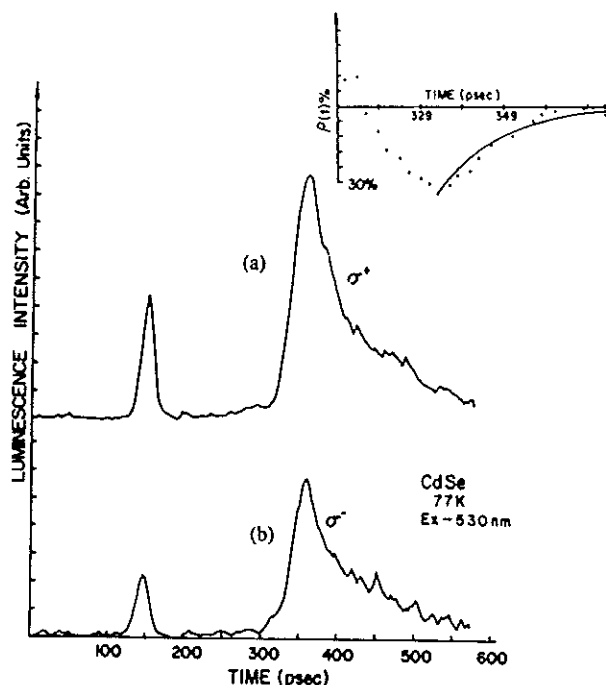


Fig. 2. The curves (a) and (b) represent photoluminescence from CdSe corresponding to σ^+ and σ^- polarizations. The excitation wavelength and polarization are 530 nm and σ^+ , respectively. The luminescence corresponds to the 680–700 nm spectral region (band edge) at 77 K. The inset is experimental data on an expanded time scale for polarization factor $\rho(t)$. The solid line is an exponential fit with $\rho(0) = 0.36$ and $T_s = 28$ ps.

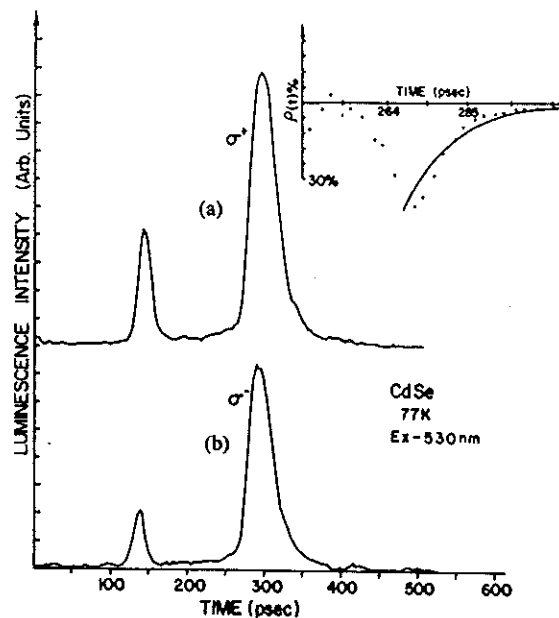


Fig. 3. The curves (a) and (b) represent photoluminescence with σ^+ and σ^- polarization. The excitation wavelength and polarization are 530 nm and σ^+ , respectively. The luminescence wavelength region is between 620–660 nm. The inset shows the theoretical fit corresponding to $\rho(0) = 0.44$ and $T_s = 24$ ps.

of the near bandgap (680–700 nm) luminescence. The inset displays the polarization factor $\rho(t)$ calculated from the data using (4) and (5) on an expanded time scale. The solid line is an exponential fit to the data with $\rho(0) = 36$

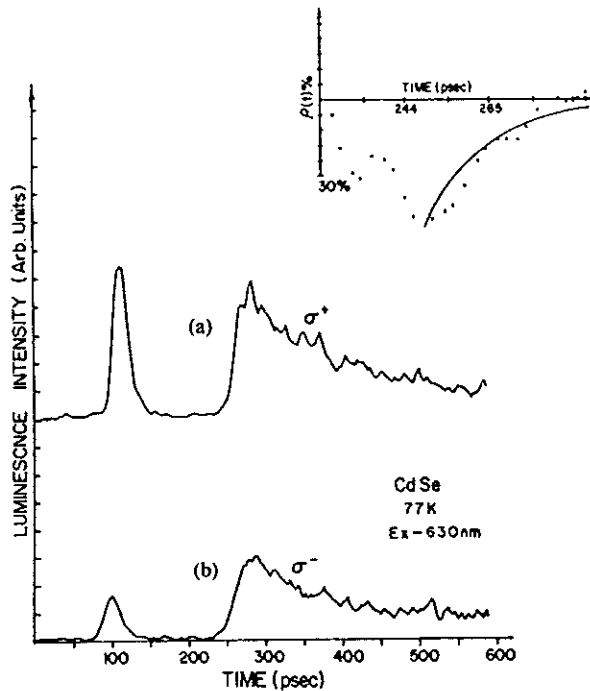


Fig. 4. The curves (a) and (b) corresponds to σ^+ and σ^- polarization with excitation wavelength of 630 nm. The excitation polarization is σ^+ . The luminescence corresponds to 680–700 nm spectral region at 77 K. The inset shows the theoretical fit corresponding to a single exponential with $\rho(0) = 0.48$ and $T_1 = 30$ ps.

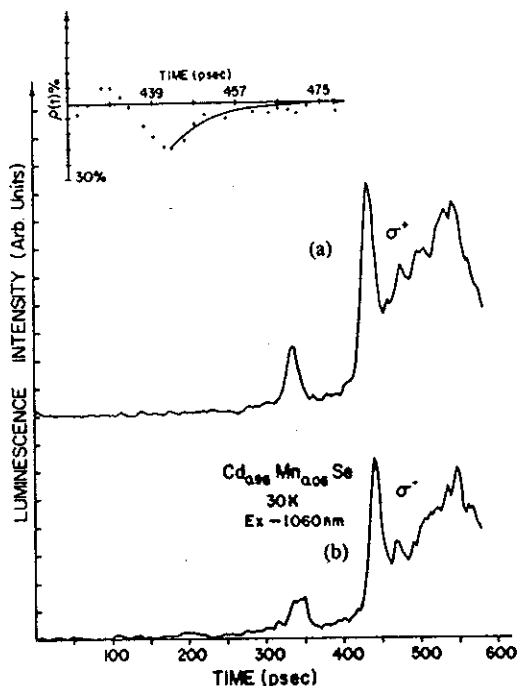


Fig. 5. The curves (a) and (b) represent spin-polarized photoluminescence from $\text{Cd}_{0.95}\text{Mn}_{0.05}\text{Se}$ at 30 K. The σ^+ and σ^- luminescence corresponds to two-photon excitation at 1060 nm and σ^+ polarization. The spectral band of the luminescence is 660 ± 10 nm. The inset curve fitting parameters are $\rho(0) = 0.2$ and $T_1 = 16$ ps.

± 5 percent and $T_1 = 28 \pm 4$ ps. Fig. 3 displays spin-polarized luminescence under similar experimental conditions for luminescence band 620–660 nm (hot luminescence). The polarization factor is $\rho(0) = 44 \pm 5$ per-

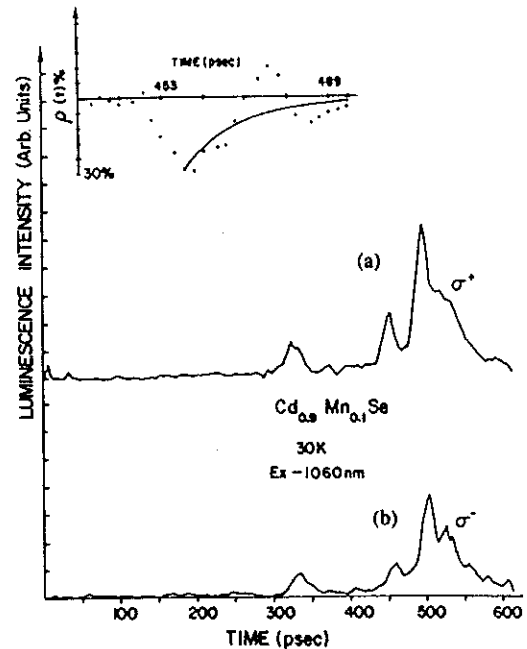


Fig. 6. The curves (a) and (b) represent spin-polarized photoluminescence from $\text{Cd}_{0.9}\text{Mn}_{0.1}\text{Se}$ at 30 K. The σ^+ and σ^- luminescence corresponds to two-photon excitation at 1060 nm and σ^+ polarization. The spectral band is 620–660 nm. The inset curve fitting parameters are $\rho(0) = 0.28$ and $T_1 = 20$ ps.

cent and the spin relaxation time is $T_1 = 24 \pm 5$ ps. Fig 4 describes band edge spin-polarized luminescence for 623 nm excitation wavelength. The corresponding values of $\rho(0)$ and T_1 are 48 ± 4 percent and 30 ± 4 ps, respectively.

B. $\text{Cd}_{1-x}\text{Mn}_x\text{Se}$

Experiments on $\text{Cd}_{1-x}\text{Mn}_x\text{Se}$ were carried out at 30 K. The bandgap in $\text{Cd}_{1-x}\text{Mn}_x\text{Se}$, as a function of x concentration, is given by [22] $E_g = 1.817 + 1.53x$ eV at a temperature of 30 K. The bandgaps for $x = 0.05$ and 0.1 are 1.89 and 1.97 eV, respectively. Two-photon excitation (1060 nm) was used to enhance the initial spin polarization. The photoluminescence for $\text{Cd}_{0.95}\text{Mn}_{0.05}\text{Se}$ was recorded with a narrow-band filter centered at 660 nm, while a broad-band filter (620–660 nm) was used for $\text{Cd}_{0.9}\text{Mn}_{0.1}\text{Se}$. The time-resolved photoluminescence shows complex behavior (Figs. 5 and 6). The second peak is delayed by about 100 ps after the first fast decay in the sample with $x = 0.05$. The second peak is delayed by ~ 50 ps in the case of $x = 0.1$. It is observed that the first luminescence peak (time-resolved) is spin-polarized, while the second peak is unpolarized. The second peak rises slowly and decays slowly in either case. Harris [23] *et al.* have observed the exchange interaction-induced red shift associated with BMP (bound magnetic polaron) formation in their time-resolved spectra. Their data suggest BMP formation time of ~ 400 ps in $\text{Cd}_{0.95}\text{Mn}_{0.05}\text{Se}$. Our result is consistent with Harris *et al.* [23], taking into account the formation time of bound exciton and BMP. The second peak is believed to be originated from the bound magnetic polaron formation (BMP) and disappears at high

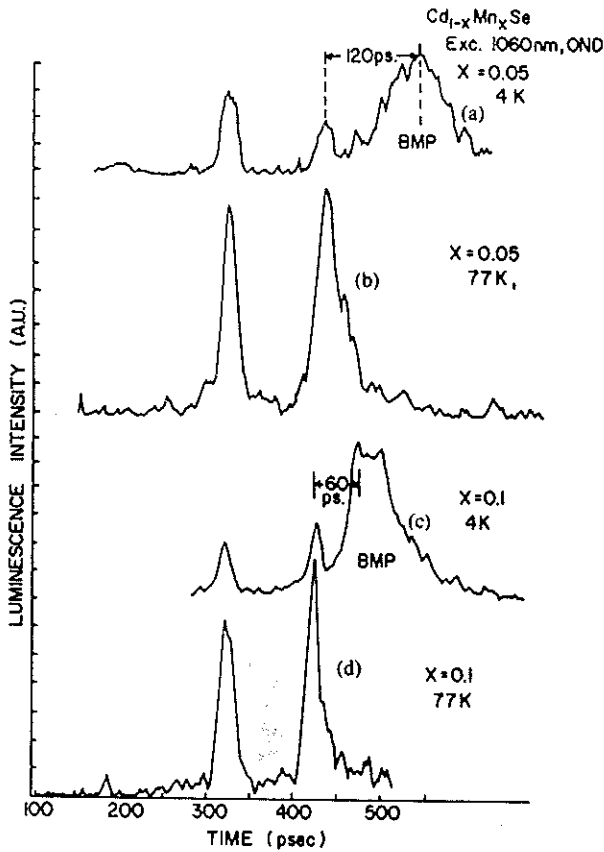


Fig. 7. The unpolarized time-resolved band edge luminescence for (a) $x = 0.05$, 4 K, (b) $x = 0.05$, 77 K, (c) $x = 0.1$, 4 K, and (d) $x = 0.1$, 77 K.

temperature (see Fig. 7). A detailed study will be discussed in a future publication [24]. The values of $\rho(0)$ and T_s for the sample with $x = 0.05$ are 18 ± 4 percent and 16 ps, respectively (see Fig. 5) and the displayed inset. The corresponding values for the sample with $x = 0.1$ are 28 ± 5 percent and 20 ps, respectively (see Fig. 6). Electron-hole recombination luminescence lifetimes derived from the first peak for $x = 0.05$ and 0.1 are about 20 ps in both samples.

THEORY

A. Spin Polarization

For most III-V and II-VI semiconductors, the transitions between the valence bands and the conduction band are principally the transitions between bands of $|P\rangle$ and $|S\rangle$ symmetries. Spin orbit interaction makes $|P\rangle \rightarrow |3/2, \pm 3/2\rangle$ and $|3/2, \pm 1/2\rangle$, and $|S\rangle \rightarrow |1/2, \pm 1/2\rangle$. The values of $\langle P|P_z|S\rangle$ are practically the same for all semiconductors and depend weakly on K (vary by a factor of two over the extent of the Brillouin zone). Fig. 1(a) displays the optical transitions for near band edge one-photon absorption, and Fig. 1(b) displays two-photon transition. The relative transition probabilities are shown in Fig. 1. The relative probability ratio [25] for σ^+ polarization absorption at 530 nm for A , B , and C valence bands to the conduction band is $\approx 3:1:2$.

Using Kane's model for band structure in semiconductors, the spin polarization factor $\rho_1(0)$ for one-photon absorption in terms of the bandgap and excitation photon energy is given by [26]

$$\rho_1(0) = \frac{(\frac{1}{2})(3\sqrt{1+y'} + 4y' - 1)}{3\sqrt{1+y'} + 1 + 2y'^2} \quad (6)$$

where $\rho_1(0)$ denotes the spin polarization factor at $t = 0$, $y' = E_g/h\omega_1$, and ω_1 is the excitation frequency.

In the case of two-photon absorption, the spin orientation factor $\rho_2(0)$ (neglecting the split-off band contribution) is given by [26]

$$\rho_2(0) = \frac{19 + \left[\frac{32y}{3} - \frac{2}{y} - \frac{4}{3}\right] [1+y]^{(3/2)} \left[\frac{3}{2} - y\right]^2}{30 + \left[\frac{32y^2}{3} + \frac{3}{8y^2}\right] [1+y]^{(3/2)} \left[\frac{3}{2} - y\right]^2} \quad (7)$$

where $\rho_2(0)$ denotes the spin polarization factor at $t = 0$, $y = E_g/2h\omega_1$, and ω_1 is the excitation frequency.

For one-photon excitations at 530 and 623 nm in the case of CdSe with a bandgap of 1.81 eV (684 nm), the initial polarization factor is calculated to be 48 and 50 percent, respectively. This is in good agreement with experiment, since the measured values for $\rho_1(0)$ are 44 and 48 percent, respectively. The bandgap of $\text{Cd}_{1-x}\text{Mn}_x\text{Se}$ for $x = 0.05$ is 1.89 eV. The calculated value of $\rho_2(0)$ is 63 percent, which compares poorly to the experimental value of 18 ± 5 percent. Similarly for $\text{Cd}_{0.9}\text{Mn}_{0.1}\text{Se}$ with a bandgap of 1.97 eV, the calculated and experimental values of $\rho_2(0)$ are 64 and 28 ± 5 percent, respectively.

B. Spin Dephasing

1) *D'yakonov and Perel' Spin Dephasing Mechanism*: The observed fast spin relaxation of free carriers in semiconductors with the wurtzite structure will be discussed within the framework of the theory proposed by D'yakonov and Perel' [4], [6] and extended by Margulis *et al.* [27]. This theory is applicable to both semiconductors, i.e., CdSe and $\text{Cd}_{1-x}\text{Mn}_x\text{Se}$. In our previous work [11] on the spin relaxation mechanisms of high-density photogenerated carriers in GaAs, we had observed that the spin relaxation is primarily due to the D'yakonov and Perel' mechanism.

According to D'yakonov and Perel' [4], [6], a semiconductor without an inversion center has a spin relaxation mechanism whose role rapidly increases in effectiveness with increasing electron energy. This mechanism involves spin splitting of the conduction band proportional to the quasi-momentum. This splitting is equivalent to an effective magnetic field acting on the spins whose direction depends on the direction of the momentum. In a GaAs crystal which has zinc blende crystal symmetry, the lack of inversion symmetry contributes a k^3 term to the conduction band electronic Hamiltonian. In a similar

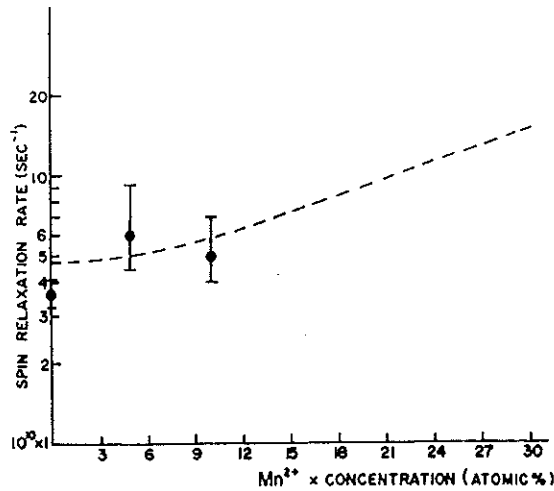


Fig. 8. The dotted line corresponds to the theoretical expression $1/T_s = Ax^2 + B$ where $1/B$ is the spin relaxation time of carriers in host CdSe. The values of A and B are as in (20). The \bullet are the experimental points.

way, the Hamiltonian describing free carriers in a semiconductor with wurtzite crystal structure has the following form [27]–[30]:

$$H = \frac{\hbar^2 k^2}{2m_e} + \gamma c \cdot (\vec{\sigma} \times \vec{k}) \quad (8)$$

where \hat{c} is a unit vector parallel to c axis, γ is a constant describing the spin splitting of the conduction band at $k \neq 0$, and $\sigma_x, \sigma_y, \sigma_z$ are the Pauli spin matrices. The role of the second term can be seen as the k -dependent effective magnetic field interacting with the carrier spins. Thus, with every collision, the effective magnetic field changes its direction, and the spin component changes its sign (dephasing), provided that the precession time is longer than the collision time (slow precession and high collision rate).

Using (8), Margulis *et al.* have shown that, for a strongly degenerate carrier distribution, the spin relaxation rate is given by [27]

$$\frac{1}{T_s} = \frac{16}{3} \frac{\gamma^2 m_e \xi \langle \tau \rangle}{\hbar^4} \quad (9)$$

where ξ is the Fermi energy, $\langle \tau \rangle$ is the collision time, and m_e is the effective mass of the electron. For a highly degenerate carrier distribution, the Fermi energy is expressed in terms of the carrier density N as

$$\xi \sim \frac{\hbar^2 ((3\pi^2 \cdot N)^{2/3})}{2m_e} \quad (10)$$

For the estimated carrier density of $5 \times 10^{18}/\text{cm}^3$, $\xi = 72$ meV. The value of γ has been measured [30] (2.56×10^{-31} J · m) in CdS using spin-flip Raman scattering. The upper limit on γ set by Hopfield [28], [29] in the case of CdSe is on the order of $(1-3) \times 10^{-31}$ J · m. We have used the value of γ measured in CdS for our order of magnitude calculation.

Using $m_e = 0.13m_0$, $\gamma = 2.56 \times 10^{-31}$ J · m, and a collision time $\langle \tau \rangle$ of 1×10^{-14} s, the expression for the

spin relaxation rate reduces to

$$\frac{1}{T_s} = 6.67 \times 10^{11} \xi \quad (11)$$

where the Fermi energy ξ is in eV. This implies that the spin relaxation time is 21 ps for a carrier concentration of $5 \times 10^{18}/\text{cm}^3$ ($\xi = 0.072$ eV), which is quite close to the measured values of ~ 26 ps. The calculated spin relaxation times for estimated carrier densities of $2 \times 10^{18}/\text{cm}^3$ and $8 \times 10^{18}/\text{cm}^3$ are 38 and 15 ps, respectively.

The temperature of the lattice does not play any significant role as long as the carriers are highly degenerate. This is due to the averaging of spin relaxation rate over a Fermi thermal distribution. We have observed almost no spin relaxation dependence on laser excitation intensities. To account for this, we believe a rapid diffusion [31], [32] of carriers from the photoexcited region takes place during the laser pulse, making the carrier concentration $5 \times 10^{18}/\text{cm}^3$ independent of excitation power within the excitation fluence ($4.25 \times 10^{27} - 1.29 \times 10^{26}/\text{cm}^2 \cdot \text{s}$). It is difficult to estimate the exact carrier concentration. The following experimental observations support this conclusion. Excitons are formed earlier than predicted by the Mott criterion from free $e-h$ plasma, no shift in the Fermi level [32], [33] as a function of excitation power was evident from the time-integrated luminescence spectra observed under high excitation laser pulses, and no appreciable change in the Auger recombination rate [32], [34] ($\sim N^2$) was observed at various excitation fluences. From time-resolved carrier temperature study [32] made at room temperature, the carrier temperature T_e is established to be < 1000 K within 30 ps. Furthermore, at 77 K, the carriers will cool much more rapidly. Hence, the criterion for a degenerate thermal distribution, i.e., $\xi/K_B T_e > 1$ at $\xi = 72$ meV, is justified.

2) *Spin-Localized Spin Exchange Dephasing Mechanism*: Ultrafast spin relaxation and the initial small spin alignment in $\text{Cd}_{1-x}\text{Mn}_x\text{Se}$ is an indication of rapid spin exchange of carrier spins with Mn^{2+} localized spins of $S = 5/2$. In wide gap semi-magnetic semiconductors, the splitting of the conduction band is given by [35]

$$\Delta E_c(H, T) = N_0 \cdot \alpha \cdot x \langle S_z \rangle \quad (12)$$

where $N_0 \alpha$ (200 meV) is the exchange parameter between the conduction s and $\text{Mn}^{2+} 3d^5$ states, x is the mole fraction of Mn atoms, and $\langle S_z \rangle$ is the mean spin component along the external magnetic field. At very low temperatures, x is replaced by \bar{x} in order to account for an anti-ferromagnetic interaction [36], [37] between Mn^{2+} ions. This will be ignored here as the temperatures are greater than $T_{AF} \approx 3$ K. Heiman *et al.* [37] have observed a zero-field spin-flip Stokes energy of 1 meV ($x = 0.1$) for lattice temperatures (1.9–28 K). The zero-field spin-flip energy for $x = 0.05$ is 0.5 meV [35]. These values can be used for the exchange energy between free electron and Mn^{2+} ions, even though these spin-flip measurements

are typically for donor bound electrons. This implies that an electron is scattered by an Mn^{2+} ion with net statistical spin of $\langle S_z \rangle = 0.05$ instead of $5/2$. Assuming a spin field dependence given by

$$\langle S_z(r) \rangle = \left(\frac{5}{2}\right) \exp -\left(\frac{r}{a'}\right)^2 \quad (13)$$

due to a localized electronic spin of strength $5/2$ where a' is the radius of the ion and r is the distance measured from the center of the ion, we have calculated the distance at which the $\langle S_z \rangle = 0.05$. Assuming an Mn^{2+} ionic radius [38] of 1.0 \AA , the estimated statistical distance measured from an Mn^{2+} ion for spin-flip scattering is 1.88 \AA ("a"). With these specified numbers in mind, we can apply the theory of D'yakonov and Perel' [39] for optical orientation in a system of donor bound electrons and lattice nuclei in semiconductors. They have calculated the effective magnetic field due to the hyperfine interaction between localized electronic spins and lattice nuclei as

$$H_c = (\mu_0 \bar{g})^{-1} \Omega_0 \left(\sum_{n=1}^{\infty} \right) (|\psi(r_n)|^2 A_{AFN} S_n) \quad (14)$$

where μ_0 is the Bohr magneton, \bar{g} is the effective g factor, Ω_0 is the volume of the unit cell, A_{AFN} is the hyperfine interaction coefficient, S_n is the nuclear spin of the n th nucleus, and $\psi(r_n)$ is the wave function of donor bound electrons at the n th nucleus. The wave function for the localized electronic state takes the form $\psi(r) = 1/\sqrt{(\pi a^3)} e^{-r/a}$. The theory could be modified for exchange interaction. The mean-square effective field is then given by [39]

$$\langle H_c^2 \rangle = \left(\frac{25\pi}{128}\right) \cdot \left(\frac{xN_0 a^3}{(\mu_0 \bar{g})^2}\right) \cdot \Delta_{ex}^2 \quad (15)$$

for $S = 5/2$ where xN_0 is the Mn^{2+} ionic concentration (N_0 is the cation density in CdSe), and Δ_{ex} is the exchange energy. For a 10 percent Mn^{2+} concentration, xN_0 is $\approx 1.8 \times 10^{21}/\text{cm}^3$ for a unit volume of $396 (\text{ \AA}^3)$ with wurtzite lattice parameters of $b = 4.3 \text{ \AA}$ and $c = 7 \text{ \AA}$.

This theory is applicable to free electron exchange interaction provided "a" is identified as the interaction distance parameter. The precession frequency is given by

$$\omega_c = \frac{\mu_0 \bar{g} \sqrt{\langle H_c^2 \rangle}}{\hbar} \quad (16)$$

and the spin relaxation rate is given by

$$\frac{1}{T_s} = \left(\frac{1}{9}\right) \omega_c^2 \tau_c \quad (17)$$

where τ_c is the collision time for electron- Mn^{2+} ion small angle scattering [6], [10].

The effective \bar{g} value derived from the mean field theory is expressed [37] in terms of Mn^{2+} concentration as

$$\bar{g} = g^* + \frac{35 \cdot x \cdot \alpha \cdot N_0}{12 \text{ K}(T + T_{AF})} g_{\text{Mn}} \quad (18)$$

where $g^* = 0.5$ is for free carriers in n-CdSe, T_{AF} is the temperature corresponding to antiferromagnetic interaction, and $g_{\text{Mn}} = 2.0$ for Mn^{2+} ions. $N_0 = 1.8 \times 10^{22}/\text{cm}^3$ is the cation density in CdSe. Lattice heating is negligible, and at 30 K, the values of effective \bar{g} for $x = 0.05$ and 0.1 are 1.6 and 47.2 , respectively.

The estimate of collision time of free electrons with magnetic ions requires a value of mean free path. It has been pointed out that for a Born approximation calculation [37] with $\alpha N_0 \sim 0.2 \text{ eV}$, the mean free path is given by

$$\lambda \approx \left(\frac{1}{x}\right) \left(\frac{m_0}{m}\right)^2 10^{-6} \quad (19)$$

where λ is expressed in cm. For an Mn concentration of 10 percent ($x = 0.1$), the mean free path is calculated to be $6 \times 10^{-4} \text{ cm}$. Assuming a Fermi velocity of $4.5 \times 10^7 \text{ cm/s}$ corresponding to the Fermi energy of 72 meV , one calculates a collision time of $\sim 14 \text{ ps}$. Hence, from (12), (13), and (14), we find the mean magnetic field, the precession frequency, and the spin relaxation time to be 976 G , $1.4 \times 10^{11}/\text{s}$, and 21.6 ps , respectively. In the case for the $x = 0.05$ CdMnSe sample, these numbers are 220 G , $4.8 \times 10^{10}/\text{s}$, and 90 ps , respectively.

Using (11), (12), (14), (15), and (16) and taking into account the spin relaxation mechanisms of the host crystal (CdSe) and the localized Mn^{2+} ions, the theoretical total spin relaxation rate (for $\xi = 72 \text{ meV}$) is given by

$$\frac{1}{T_s} = 1.08 \times 10^{12} (x^2) + 4.75 \times 10^{10} \quad (20)$$

in s^{-1} .

The total spin relaxation times calculated are 17 and 20 ps for $x = 0.1$ and 0.05 , respectively. These values are in reasonable agreement with our measurements.

DISCUSSION

A. CdSe (Host Crystal $x = 0$)

The spin polarization factors and spin relaxation times for CdSe measured for various luminescence bands with different one-photon excitation energies are in excellent agreement with theory.

For GaAs, the valence bands $|3/2, \pm 3/2\rangle$ and $|3/2, \pm 1/2\rangle$ are degenerate at the center of Brillouin zone; this results in the luminescence polarization factor of ≈ 25 percent (for a selection rule allowed spin polarization factor of ≈ 50 percent). In CdSe, the valence band degeneracy is removed by crystal field splitting $\Delta_{cr} \approx 26 \text{ meV}$ at $k = 0$. At our excitation levels, the hole Fermi level is about 24 meV , which allows only the $|3/2, \pm 3/2\rangle$ (A valence) band holes to participate in the luminescence process. The B and C bands are occupied by electrons. In this case, the luminescence polarization factor is the same as the free carrier spin polarization factor because the $|3/2, \pm 1/2\rangle$ band does not participate in the recombination.

The luminescence bands selected for 530 nm excitation are in the 620–660 nm and 680–700 nm wavelength regions. The luminescence band for 630 nm excitation in our experiment is 15 meV above the bottom of conduction band with a luminescence region of 680–700 nm. The difference between these pulse excitation conditions is that the split-off valence band Γ_7 is pumped by 530 nm excitation, while for 623 nm excitations, it is precluded due to the energy difference. The near band edge (15 meV above bandgap) spin polarization factor is defined to be ρ_{BE} .

The polarization factor ρ , measured near the excitation energies, for 530 and 623 nm excitation are 44 ± 5 and 48 ± 4 percent (as shown in Figs. 3 and 4), respectively. This agrees well with the theoretical values of 48 and 50 percent, respectively. To qualitatively understand the relationship between these ρ 's, the effect of the split-off valence band (Γ_7) has been neglected for 530 nm excitation. This is a reasonable assumption because the density of states is about a factor of 10 smaller for Γ_7 than for the Γ_9 valence band. This generates fewer carriers in the conduction band edge due to the transition from the Γ_7 valence band. The effect of this transition is to depolarize the spin alignment of the selection rules [25]. This effect is less than 3 percent, and contributes to the observed band edge 680–700 nm (15 meV above the bandgap) spin polarization factor $\rho_{BE}(0)$ of 36 ± 5 percent observed under 530 nm one-photon excitation (Fig. 2). The observed hot electron polarization factor of 44 ± 5 percent (Fig. 3) is somewhat larger than the band edge electron spin polarization factor. This observation is consistent with the split-off valence band transition argument given above, although the difference is larger than expected. The observed delay time between the hot and band edge luminescence is ≈ 6 ps for 530 nm excitation and less than 3 ps for 623 nm excitation. This can explain the lower value $\rho_{BE}(0)$ if we allow for the spin relaxation ($\rho_{BE}(0) = \rho(0) \exp(-2t/T_s)$) during 6 ps with a spin relaxation lifetime of 30 ps. This result is consistent with 623 nm (1.986 eV) excitation, as the observed value for $\rho_{BE}(0)$ of 48 percent is larger than 530 nm excitation $\rho_{BE}(0)$ value of 36 percent. The spin relaxation times obtained in the hot luminescence region (620–660 nm) and the band edge region (680–700 nm) are 25 ± 5 and 28 ± 5 ps, respectively, for 530 nm excitation. The hot carriers have 15LO phonon excess energy compared to the band edge carriers. This means that the electron-LO phonon scattering additional channel is available for the hot electron energy relaxation and for spin relaxation. Since experimentally we do not find any significant difference between the spin relaxation times for different carrier energies, we conclude that the LO phonon emission does not play a major role in the spin relaxation process. The measurements of spin polarization factors are also in agreement with the above conclusion as the LO phonon emission time is $\sim 10^{-12}$ s compared to $e-e$ or $e-h$ collision times of $\sim 10^{-14}$ s.

The measured value of spin relaxation time (≈ 25 ps) is in good agreement with theory (21 ps) The theoretical

spin relaxation times are sensitive to the exact knowledge of values of γ and Fermi level ξ . The spin relaxation times are a little longer for near edge carrier (≈ 30 ps) compared to near excitation carriers (25 ps). This is expected as the mechanism is effective for large k . Spin relaxation times and initial polarization factors are the same for the high-resistivity ($10^6 \Omega \cdot \text{cm}$) and low-resistivity ($12 \Omega \cdot \text{cm}$) samples, which indicates that the electron-*Se* vacancy scattering rate is significantly smaller as compared to electron-hole or electron-electron scattering rates ($\tau_c \sim 10^{-14}$ s). The observed band edge luminescence ($\sigma^+ + \sigma^-$) shows two-component decay (Fig. 2), whereas the spin polarization $(\sigma^+ - \sigma^-)/(\sigma^+ + \sigma^-)$ is observed only in the fast component. The recombination luminescence lifetimes (fast component) are short ≈ 45 ps in the low-resistivity sample (n type) as compared to ≈ 70 ps in a high-resistivity sample. This fast component is essentially due to Auger recombination. The difference in the lifetimes is a measure of hole capture rate at the hole capture centers existing in low-resistivity samples (only n type CdSe could be grown). However, the observed spin relaxation times are about the same in the high- and low-resistivity samples due to the lattice inherent DP mechanism. Conduction electron Raman spin-flip measurements in CdS gives [15] an estimate of 10^{-11} s for the spin relaxation time, which should be on the order of magnitude expected for CdSe because of similarity in crystal structure. The very fact that experimentally we observe ~ 50 percent luminescence polarization at $t = 0$ justifies the assumption that even in CdSe ($x = 0$), the valence holes depolarize within 10^{-13} s. Warnock [19] *et al.* have observed this fast spin relaxation of holes in $\text{Cd}_{1-x}\text{Mn}_x\text{Se}$ ($x = 0.05$ and $x = 0.1$) for above bandgap excitation.

B. $\text{Cd}_{1-x}\text{Mn}_x\text{Se}$ ($x = 0.05$ and 0.1)

The observed values of the two-photon spin polarization factor $\rho_2(0)$ of 20 percent for $\text{Cd}_{0.95}\text{Mn}_{0.05}\text{Se}$ and 28 percent for $\text{Cd}_{0.9}\text{Mn}_{0.1}\text{Se}$ are not consistent with the theoretical values of 63 and 64 percent, respectively (see Table I). This is believed to be due to the existence of Mn^{2+} excited states [40], [41] (4G) in the conduction band. Angle-resolved ultraviolet photoemission spectroscopy [42] studies had clearly indicated strong hybridization of Mn^{2+} d levels with p -like states in the valence band. In such a case, the optical transition is from a mixed ($p\text{-}A_1$) valence band to a mixed ($s\text{-}^4A_1$, 4E , 4T_1 , and 4T_2) conduction band. These mixed levels may play an important role in reducing the polarization factor $\rho_2(0)$ by modifying the selection rules. The theoretical agreement of spin relaxation times in $\text{Cd}_{1-x}\text{Mn}_x\text{Se}$ is subject to our approximation in the calculations of the collision distance a and scattering time τ_c . However, in the case of $\text{Cd}_{1-x}\text{Mn}_x\text{Se}$ samples, a confirming trend of shorter spin relaxation time with increasing x has been established through our experiments, although the exact relationship between T_s and x has not been well established (see (20) and Fig. 8). It is necessary to measure high concentration samples with higher temporal resolution in order to obtain the exact de-

TABLE I
THE EXPERIMENTAL CONDITION (EXCITATION WAVELENGTH,
TEMPERATURE, AND LUMINESCENCE BAND), MEASURED VALUES OF ρ_0 AND
 T_1 , AND THEORETICAL VALUES OF ρ_0 AND T_1 ARE TABULATED FOR
 $Cd_{1-x}Mn_xSe$

EXPERIMENTAL CONDITIONS and MEASUREMENTS					THEORETICAL VALUES	
SAMPLE	ρ_0 (%)	T_1 (pscc)	EXCITATION WAVELENGTH (nm)	PHOTO LUMINESCENCE WAVELENGTH (nm)	ρ_0 (%)	T_1 (pscc)
$CdSe$ $x=0$ (77K)	44±5	24±5	530	620 - 660	48	21
	36±5	28±5	530	680 - 700	32	21
	48±4	30±4	630	680 - 700	50	21
$Cd_{0.95}Mn_{0.05}Se$ (30K)	18±4	16±5	1060	660 ± 10	63	20
$Cd_{0.9}Mn_{0.1}Se$ (30K)	28±5	20±5	1060	620 - 660	64	17

pendence of spin relaxation time on magnetic concentration.

The free carrier luminescence (first peak) is polarized and BMP luminescence (second peak) shows almost zero polarization. This is consistent with Warnock *et al.* [19] (steady state $\rho \sim 1$ percent), which is due to fast relaxation of free carriers ($e-h$) within 30 ps for above bandgap excitation. Therefore, they observed the near-zero polarization of BMP. It is known [39] that the spin state of the nuclei changes due to the exchange interaction with the spin-polarized electrons. Since the spin exchange time involved is $\sim 10^{-6}$ s, this cannot influence the spin relaxation rate of free carriers during the lifetime of the free carriers (40 ps). Thus, the observed increase in spin relaxation time (20 ps in $Cd_{0.9}Mn_{0.1}Se$ versus 16 ps in $Cd_{0.95}Mn_{0.05}Se$) is not due to the transfer of angular momentum from Mn^{2+} spins to carrier spin system. Raman spin-flip scattering (RSFS) line widths is an indirect measure of spin decreasing times. For $Cd_{1-x}Mn_xSe$, data on conduction electron Raman spin-flip scattering time are not available. For localized bound states (i.e., BMP), the Raman spin-flip line width broadening is partly due to large inhomogeneities of the environment. Hence, the observed line width of $\sim 8 \text{ cm}^{-1}$ (1 meV for $x = 0.1$) [37] is enhanced and should not be taken to calculate the spin relaxation time. This will give an underestimate $< 10^{-12}$ s. Taking this factor into account, we believe our direct measurements are more accurate than the dephasing time established by the RSFS measurements.

The observed spin relaxation times in $Cd_{1-x}Mn_xSe$ could be explained in terms of D'yakonov and Perel' mechanisms since in other spin relaxation mechanisms, i.e., Elliot and Yafet [7], [10], Bir *et al.* [8], and Kleinman and Miller [9], virtual photon mechanisms are at least one order of magnitude slower. Since the different mechanisms depend on the levels of carrier density and temperature, a large range of excitation powers is needed to understand and quantitatively describe which spin relaxation process dominates in $Cd_{1-x}Mn_xSe$. Our present single-shot laser system precludes a density dependence

study due to a lack of good signal-to-noise ratio at low excitation.

ACKNOWLEDGMENT

We thank Prof. J. Spalek for helpful comments on the manuscript.

REFERENCES

- [1] R. L. Bell, *Negative Electron Affinity Devices*. Oxford: Clarendon, 1973.
- [2] G. Lampel, "Nuclear dynamic polarization by optical electronic saturation and optical pumping in semiconductors," *Phys. Rev. Lett.*, vol. 20, pp. 491-493, 1968.
- [3] R. R. Parsons, "Band-to-band optical pumping in solids and polarized photoluminescence," *Phys. Rev. Lett.*, vol. 23, pp. 1152-1154, 1969.
- [4] M. I. D'yakonov and V. I. Perel', "Spin orientation of electrons associated with the interband absorption of light in semiconductors," *Sov. Phys. JETP*, vol. 33, pp. 1053-1059, 1971.
- [5] D. Long, *Energy Bands in Semiconductors*. New York: Interscience, 1986, ch. 7.
- [6] M. I. D'yakonov and V. I. Perel', "Spin relaxation of conduction electrons in noncentrosymmetric semiconductors," *Sov. Phys. Solid State*, vol. 13, pp. 3023-3026, 1972.
- [7] R. J. Elliott, "Theory of the effect of spin-orbit coupling on magnetic resonance in some semiconductors," *Phys. Rev.*, vol. 96, pp. 266-279, 1954.
- [8] G. L. Bir, A. G. Aronov, and G. E. Pikus, "Spin relaxation of electrons due to scattering by holes," *Sov. Phys. JETP*, vol. 42, pp. 705-712, 1976.
- [9] D. A. Kleinman and R. C. Miller, "Relaxation of optically pumped electron spin through a virtual photon experimental evidence in heavily Zn-doped GaAs," *Phys. Rev. Lett.*, vol. 46, pp. 68-71, 1981.
- [10] G. Fishman and G. Lampel, "Spin relaxation of photoelectrons in p-type gallium arsenide," *Phys. Rev.*, vol. B16, pp. 820-831, 1977.
- [11] R. J. Seymour, M. R. Junnarkar, and R. R. Alfano, "Spin relaxation of photogenerated degenerate electron distribution in GaAs," *Phys. Rev.*, vol. B24, pp. 3623-3625, 1981.
- [12] A. H. Clark, R. D. Burnham, D. J. Chadi, and R. M. White, "Spin relaxation of conduction electrons in GaAs," *Solid State Commun.*, vol. 20, pp. 385-387, 1976.
- [13] V. B. Vekua, R. I. Dzhoiev, B. P. Zakharchenya, and V. G. Fleisher, "Hanle effect in optical orientation of electrons in n-type semiconductors," *Sov. Phys. Semicond.*, vol. 10, pp. 210-213, 1976.
- [14] G. Lampel, "Optical pumping in semiconductors," in *Proc. 12th Int. Conf. Phys. Semiconductors*, M. H. Pikhun, Ed. Stuttgart: Teubner, 1974, pp. 743-750.
- [15] P. A. Fleury and J. F. Scott, "Spin-flip Raman scattering from conduction electrons in CdS and ZnSe," *Phys. Rev.*, vol. B3, p. 1979, 1971.
- [16] J. F. Scott, T. C. Damen, and P. A. Fleury, "Linewidths and two-electron processes in spin-flip Raman scattering from CdS and ZnSe," *Phys. Rev.*, vol. B6, pp. 3856-3864, 1972.
- [17] R. J. Seymour and R. R. Alfano, "Time resolved measurement of the electron-spin relaxation kinetics in GaAs," *Appl. Phys. Lett.*, vol. 37, pp. 231-233, 1980.
- [18] J. K. Furdyna, "Diluted magnetic semiconductors: An interface of semiconductor physics and magnetism," *J. Appl. Phys.*, vol. 53, pp. 7637-7643, 1982.
- [19] J. Warnock, R. N. Kershaw, D. Ridgley, K. Dwight, A. Wold, and R. R. Galazka, "Optical orientation of excitons in (Cd, Mn)Se and (Cd, Mn)Te," *Solid State Commun.*, vol. 54, pp. 215-219, 1985.
- [20] P. Y. Lu, P. P. Ho, and R. R. Alfano, "Nd: phosphate glass mode-locked oscillator and amplifier system," *IEEE J. Quantum Electron.*, vol. QE-15, pp. 406-407, 1979.
- [21] R. J. Seymour, "Electron spin and energy relaxation in highly excited GaAs," New York Univ., New York, NY, unpublished thesis, 1981.
- [22] J. Stankiewicz, "Electroreflectance studies in Mn, Cd_{1-x}Se," *Phys. Rev.*, vol. B27, pp. 3631-3636, 1983.
- [23] J. H. Harris and A. V. Nurmikko, "Formation of the bound magnetic polaron in (Cd, Mn)Se," *Phys. Rev. Lett.*, vol. 51, pp. 1472-1475, 1983.
- [24] M. R. Junnarkar, "Picosecond and steady state spectroscopy of

- wurtzite semimagnetic semiconductor $Cd_{1-x}Mn_xSe$," City Univ. New York, New York, NY, unpublished thesis, 1986.
- [25] E. J. Johnson, R. J. Seymour, and R. R. Alfano, "Photoluminescence of spin-polarized electrons in semiconductors," in *Semiconductors Probed by Ultrafast Laser Spectroscopy, Vol. II*, R. R. Alfano, Ed. New York: Academic, 1984, pp. 199-241.
- [26] E. L. Ivchenko, "Two-photon absorption and optical orientation of free carriers in cubic crystals," *Sov. Phys. Solid State*, vol. 14, pp. 2942-2946, 1972.
- [27] A. D. Margulis and V. A. Margulis, "Spin relaxation of free carriers in semiconductors with the wurtzite structure," *Sov. Phys. Semicond.*, vol. 18, pp. 305-308, 1984.
- [28] J. J. Hopfield, "Exciton states and band structure in CdS and CdSe," *Phys. Rev.*, vol. 32, pp. 2277-2281, 1961.
- [29] G. D. Mahan and J. J. Hopfield, "Optical effects of energy terms linear in wave vector," *Phys. Rev.*, vol. 135, pp. A428-A433, 1964.
- [30] R. Romestain, S. Geschwind, and G. E. Devlin, "Measurement of the linear k term in a polar crystal (CdS) by spin-flip Raman scattering," *Phys. Rev. Lett.*, vol. 39, pp. 1583-1586, 1977.
- [31] N. J. Frigo, H. Mahr, and D. J. Erskine, "Application of a two-wavelength picosecond laser to semiconductors," *IEEE J. Quantum Electron.*, vol. QE-18, pp. 192-198, 1982.
- [32] M. R. Junnarkar and R. R. Alfano, "Photogenerated high-density electron-hole plasma energy relaxation and experimental evidence for rapid expansion of the electron-hole plasma in CdSe," *Phys. Rev.*, vol. B34, pp. 7045-7062, 1986.
- [33] J. I. Pankove, *Optical Processes in Semiconductors*. New York: Dover, 1971, p. 129.
- [34] J. S. Blakemore, *Semiconductor Statistics*. New York: Pergamon, 1962, p. 214.
- [35] M. Nawrocki, R. Planel, and G. Fishman, "Exchange-induced spin-flip Raman scattering in a semimagnetic-semiconductor," *Phys. Rev. Lett.*, vol. 46, pp. 735-738, 1981.
- [36] D. Heiman, "Magnetically tunable stimulated emission from recombination radiation in $(Cd, Mn)Se$," *Appl. Phys. Lett.*, vol. 42, pp. 775-776, 1983.
- [37] D. Heiman, P. A. Wolff, and J. Warnock, "Spin-flip Raman scattering, bound magnetic polaron, and fluctuations in $(Cd, Mn)Se$," *Phys. Rev.*, vol. B27, pp. 4848-4860, 1983.
- [38] A. Beiser, *Perspectives of Modern Physics*. New York: McGraw-Hill, 1969, p. 424.
- [39] M. I. D'yakonov and V. J. Perel', "Optical orientation in a system of electrons and lattice nuclei in semiconductors theory," *Sov. Phys. JETP*, vol. 38, pp. 177-183, 1974.
- [40] M. P. Vecchi, W. Giriat, and L. Videla, "Photoluminescence studies of the Mn^{2+} d -levels in $Cd_{1-x}Mn_xTe$," *Appl. Phys. Lett.*, vol. 38, pp. 99-101, 1981.
- [41] R. Y. Tao, M. M. Moriwaki, W. M. Becker, and R. R. Galazka, "Comparison of excitation spectra of 1.2 and 2.0 eV photoluminescence bands in $Cd_{1-x}Mn_xTe$ for $0.4 < x \leq 0.7$," *J. Appl. Phys.*, vol. 53, pp. 3772-3776, 1982.
- [42] P. Oelhafen, M. P. Vecchi, J. L. Freeouf, and V. L. Moruzzi, "The delocalized d -electrons in the semimagnetic alloy $Cd_{1-x}Mn_xTe$," *Solid State Commun.*, vol. 44, pp. 1547-1550, 1982.

Mahesh R. Junnarkar received the B.Sc. degree in physics from the University of Bombay, India, in 1976 and the M.Sc. degree in physics from the Indian Institute of Technology, Kampur, in 1978. He finished his graduate work (Ph.D.) at the Institute for Ultrafast Spectroscopy and Lasers (IUSL), City College of New York, New York, NY, in 1986.

Currently, he is working on time-resolved spin/energy relaxation measurements on quantum wells at IUSL using a CPM dye laser four-stage amplifier system. His future plans include studies of transient electrical responses of superconductors.

R. R. Alfano, for a photograph and biography, see this issue, p. 364.

J. K. Furdyna, photograph and biography not available at the time of publication.